Mitochondrion 69 (2023) 83–94

Contents lists available at ScienceDirect

Mitochondrion

journal homepage: www.elsevier.com/locate/mito

How hot can mitochondria be? Incubation at temperatures above 43 °C induces the degradation of respiratory complexes and supercomplexes in intact cells and isolated mitochondria

Raquel Moreno-Loshuertos [a,b], Joaquín Marco-Brualla [a,c], Patricia Meade [a,b], Ruth Soler-Agesta [a], José A. Enriquez [d,e], Patricio Fernández-Silva [a,b,*]

[a] Department of Biochemistry and Molecular and Cellular Biology, University of Zaragoza, 50009 Zaragoza, Spain
[b] Institute for Biocomputation and Physics of Complex Systems (BIFI), Zaragoza, Spain
[c] Peaches Biotech Group, Madrid, Spain
[d] Fundación Centro Nacional de Investigaciones Cardiovasculares Carlos III, Madrid, Spain
[e] Centro de Investigaciones Biomédicas en Red en Fragilidad y Envejecimiento Saludable, Madrid, Spain

ARTICLE INFO

Keywords:
Mitochondria
Respiratory complex
Supercomplex
Hyperthermia
Stability
Temperature

ABSTRACT

Mitochondrial function generates an important fraction of the heat that contributes to cellular and organismal temperature maintenance, but the actual values of this parameter reached in the organelles is a matter of debate. The studies addressing this issue have reported divergent results: from detecting in the organelles the same temperature as the cell average or the incubation temperature, to increasing differences of up to 10 degrees above the incubation value. Theoretical calculations based on physical laws exclude the possibility of relevant temperature gradients between mitochondria and their surroundings. These facts have given rise to a conundrum or paradox about hot mitochondria.

We have examined by Blue-Native electrophoresis, both in intact cells and in isolated organelles, the stability of respiratory complexes and supercomplexes at different temperatures to obtain information about their tolerance to heat stress. We observe that, upon incubation at values above 43 °C and after relatively short periods, respiratory complexes, and especially complex I and its supercomplexes, are unstable even when the respiratory activity is inhibited. These results support the conclusion that high temperatures (>43 °C) cause damage to mitochondrial structure and function and question the proposal that these organelles can physiologically work at close to 50 °C.

1. Introduction

Temperature is a key factor for life since it conditions virtually all biological activities, including ATP production, and its control in endotherms is considered an evolutionary advantage allowing higher metabolic efficiency (Clarke, 2017; Clarke and Pörtner, 2010). Temperatures over the physiological limits (heat stress) can damage cell structure and function leading to cell death (Zhao et al., 2006; Slimen et al., 2014), and are involved in some pathological conditions as well as being used as an anticancer therapeutic strategy (Qian et al., 2004; Wust et al., 2002). Knowing those limits and where they reside has relevant implications in understanding and preventing unwanted cell damage and in managing hyperthermia-based treatments.

Mitochondria are the most important source of heat, mainly through the activity of the OXPHOS system located in the inner membrane and the associated proton leak (Clarke and Pörtner, 2010; Rolfe and Brown, 1997). Given the elevated concentration of OXPHOS complexes at the cristae and the presence of a double membrane limiting the organelles, it could be expected that the temperature in mitochondria could reach values above those of the surrounding cell environment, although how much higher is a matter of debate (Bafou et al., 2014; Lane, 2018; Macherel et al., 2021; Fahimi and Matta, 2022). The possibility to

Abbreviations: AA, antimycin A; BN-PAGE, Blue-Native polyacrylamide gel electrophoresis; CI-CV, complex I-complex V; DAB, diaminobenzidine; IGA, in gel activity assay; MTY, Mito Thermo Yellow; NBT, nitro tetrazolium blue; RC, respiratory complex; ROS, reactive oxygen species; SC(s), supercomplex(es); WB, western blot.

* Corresponding author at: Department of Biochemistry and Molecular and Cellular Biology, University of Zaragoza, 50009 Zaragoza, Spain.
E-mail address: pfsilva@unizar.es (P. Fernández-Silva).

https://doi.org/10.1016/j.mito.2023.02.002
Received 22 September 2022; Received in revised form 25 January 2023; Accepted 4 February 2023
Available online 9 February 2023

measure intracellular heat production and temperature variations would be of great interest both to basic and applied science. However, this determination in living cells is challenging and, although several methods have been reported (Okabe et al., 2018; Sakaguchi et al., 2015), so far there is not an established and generally recognised approach. Thus, the actual levels and the physiological limits of temperature reached inside the mitochondria remain unresolved questions (Lane, 2018; Macherel et al., 2021; Fahimi and Matta, 2022) with controversy and divergent results (Chrétien et al., 2018; Kiyonaka et al., 2013; Nakano et al., 2017; Hayashi et al., 2015; Qiao et al., 2018; Savchuk et al., 2019; Homma et al., 2015; Huang et al., 2018; Kriszt et al., 2017).

It has been reported that, in cultured cells, functioning mitochondria reach physiologically temperatures of 48–50 °C, more than 10 °C above the externally applied value (38 °C) (Chrétien et al., 2018). Blocking respiratory complex function by reducing mtDNA levels or using OXPHOS inhibitors such as rotenone or KCN prevented the rise in temperature, implying that it was mainly generated by OXPHOS activity (Chrétien et al., 2018). These results are surprising since they contradict theoretical considerations (Bafou et al., 2014; Lane, 2018; Macherel et al., 2021; Fahimi and Matta, 2022) and previous reports that placed mitochondrial temperatures in a lower range (Kiyonaka et al., 2013; Nakano et al., 2017; Hayashi et al., 2015; Qiao et al., 2018; Savchuk et al., 2019; Homma et al., 2015; Huang et al., 2018), giving rise to what has been called the "hot mitochondria conundrum or paradox" (Macherel et al., 2021; Fahimi and Matta, 2022).

To contribute in clarifying this "conundrum", we decided to examine the stability of respiratory complexes (RCs) and supercomplexes (SCs) at different temperatures. For this study, cultured cells and cells obtained from liver tissue as well as isolated liver mitochondria were incubated at temperatures spanning from 37 to 50 °C either in the absence or in the presence of OXPHOS inhibitors. Subsequently, the complex and SCs organization status and activity were analysed. The rational for this approach is based on the premise that the structure and function of the enzymes and complexes that work in the mitochondria, and that are directly involved in heat generation, should remain stable within the range of physiological temperatures reached in the organelles. Our findings show that RCs, and more markedly SCs, are disorganized and their activity is compromised after relatively short times at temperatures above 43 °C. These effects are observed even when the potential increase in temperature (over the incubation value) due to the OXPHOS activity is prevented by different inhibitors that block respiration. The temperature-dependent de-stabilization is similar but not identical in liver and cultured cells and also differs for the various RCs and their associations, being complex I (CI) and CI-containing SCs (CI-SCs) particularly sensitive to heat stress. The main effects of high temperatures on RCs and SCs observed in whole cells were reproduced in isolated mitochondria, indicating that they are not mediated by other cell compartments or by mitochondrial turnover. These results question the conclusion that mitochondria can operate physiologically and have an optimal function at close to 50 °C and place a limit to this value below 43 °C.

2. Results

2.1. Incubation at high temperatures preferentially affects mitochondrial function in cultured cells

The effects of different temperatures on human MDA-MB-468 (from now on MDA) cell morphology, viability and respiration capacity were determined. For this, the cells were incubated at 43, 45 and 47 °C for 1 h. The different analysis were performed immediately after this incubation and after an additional incubation or "recovery" at 37 °C. This recovery time was of 1 h for the respiration measurements and of 6 h for viability and survival analysis. In all cases the results were compared to cells kept at the standard temperature of 37 °C. After the incubation at 43, 45 and 47 °C, the cells acquired a progressively more rounded shape and smaller size although no significant detachment from the culture plate was observed. The cell viability, as determined by trypan blue exclusion assay, suffered a small and progressive reduction reaching around 75% (relative to the 37 °C sample) after incubation for 1 h at 47 °C (Fig. 1A). Similarly, cell death determination by flow cytometry after labelling to detect membrane and DNA damage revealed a mild effect since most cells were still living immediately after the different treatments (more than 85% in the case of the treatment at 47 °C relative to 37 °C) (Fig. 1B). The "recovery" period for 6 h at 37 °C allowed the cells treated at 43 and 45 °C to reach the viability and survival values of control cells (37 °C). On the contrary, the cells incubated for 1 h at 47 °C still suffered a reduction in their viability and survival rates after the 6 h recovery period (to around 60% an 70% of controls, respectively) (Fig. 1A and B).

When the respiration activity was measured, we found that both basal coupled and uncoupled (maximal) respiration were affected, in a temperature-dependent fashion, by the treatments. Thus, while in 43 °C-treated cells these parameters were not modified, they were significantly reduced at 45 °C (to around 70% of the basal respiration control values at 37 °C) and even more strongly reduced at 47 °C (to 40% of the basal respiration control values) (Fig. 1C). A further incubation at 37 °C for 1 h did not allow the high-temperature treated cells (at 45 and 47 °C) to recover the normal respiration levels (Fig. 1C). The ratio between uncoupled and coupled respiration progressively diminished from around 1.5 in control cells to around 1.2 and 1.0 in cells treated at 45 and 47 °C, respectively (Fig. S1A), suggesting either a decrease in the reserve capacity or an increased contribution of the proton leak (uncoupling) to the basal respiration. To obtain more information on these effects, we measured the inhibition of the basal respiratory rate with titrated concentrations of oligomycin after treatment at 45 and 47 °C for 1 h. This analysis showed that the oligomycin concentration needed to reach the maximum inhibition (a level around 20% of the initial respiration (without oligomycin) in all cases) was 2.8 μM for control cells (37 °C), but it was reduced to 1.6 and 0.6 μM, respectively, in the case of cells treated at 45 and 47 °C (Fig. S1B). In addition, uncoupling with DNP after the titration with oligomycin still allowed the respiration level to recover to values close to the respective average uncoupled measurement presented in Fig. 1C (Fig. S1B). This would exclude that the measured basal respiration in treated cells corresponds to uncoupled respiration in a larger proportion than in control cells. Instead, these results suggest that the cells treated at the higher temperatures, when placed again at 37 °C for the basal respiration analysis, use their remaining respiratory capacity closer to its maximum level than control cells.

The results described above indicate that the cell treatment at 45 and 47 °C, although it did induce only a modest initial effect on cell death/viability, it severely compromised mitochondrial function. These findings point to a selective or preferential damage of the organelles that eventually leads, particularly in the case of the higher temperature, to cell death in the proceeding hours. In fact, in the treatment at 47 °C, after 6 h of recovery at 37 °C there was still a decrease in the proportion of viable/surviving cells (Fig. 1A and B), suggesting that the mitochondrial damage was too severe in some cells, leading to their loss of viability.

2.2. SCs and CI are unstable at temperatures over 43 °C in intact human and mouse cultured cells

To analyse the effect of temperature on RCs and SCs stability in intact cells, human MDA and murine L929^{Balbc} cells were incubated at the control (37 °C) and at higher temperatures, up to 50 °C, for various times and in the presence or absence of OXPHOS inhibitors. After incubation of the cells, the mitochondria were purified and the RCs and their associations, following their solubilization with digitonin and separation under native conditions using Blue-Native polyacrylamide electrophoresis (BN-PAGE), were detected directly on the gels by in gel activity determination (IGA) and by western blot (WB) with the corresponding

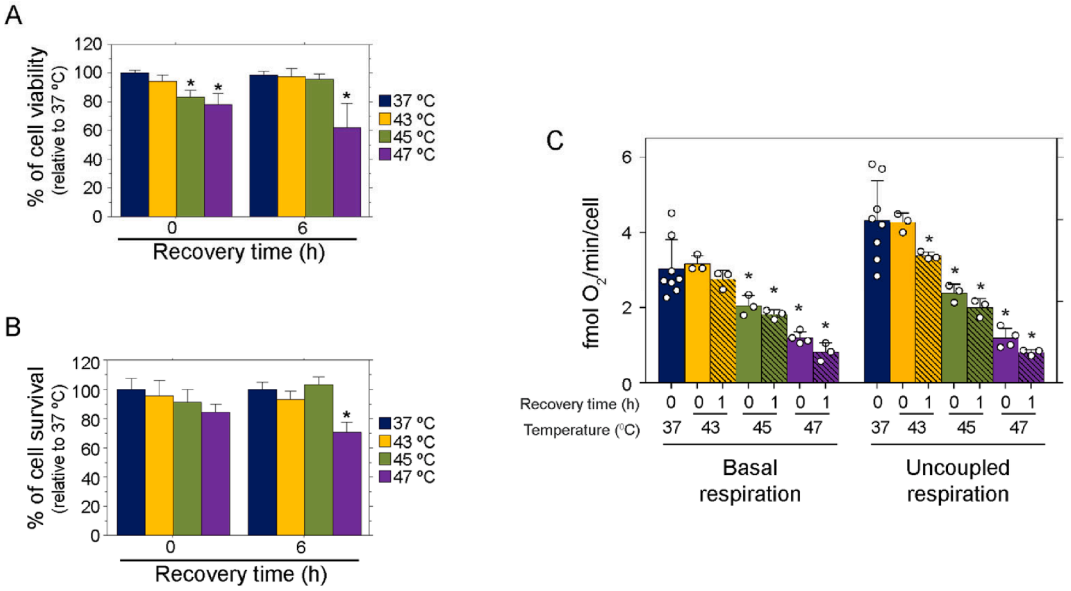

Fig. 1. Effect of temperature incubation on MDA-MB-468 cell viability, survival and respiration. A) Cell viability, measured by the trypan blue exclusion test, immediately after incubation at the indicated temperature for 1 h (Recovery (h) "0"; n = 5 for 37 °C and n = 4 for the rest), and after 6 h of additional incubation at 37 °C (Recovery (h) "6"; n = 4 for 37 °C and n = 3 for the rest). B) Cell survival measured by 7-AAD and Annexin-V-FITC staining by flow cytometry, immediately after the different temperature treatments for 1 h (Recovery "0"; n = 6 for 37 °C and n = 3 for the rest), and after 6 h of additional incubation at 37 °C ("6"; n = 5 for 37 °C and n = 3 for the rest). C) Respiration values (oxygen consumption) immediately after incubation at the indicated temperatures for 1 h and after an additional incubation at 37 °C for 1 h (Recovery (1 h)). Left: basal coupled respiration; right: uncoupled or maximal respiration. (n = 8 for 37 °C, n = 4 for 47 °C and n = 3 for the rest). * $p < 0.05$ with respect to 37 °C; see M&M for details. (For interpretation of the references to colour in this figure legend, the reader is referred to the web version of this article.)

antibodies.

We observed both quantitative and qualitative effects of incubation at high temperatures on the OXPHOS system organization status. These effects of heat stress on complex and SCs levels were both time and temperature dependent. Incubation of MDA cells for one hour at 43 °C had only a small effect on the complex I-containing SCs (CI-SCs), composed by different associations between CI + CIII and by CI + CIII + CIV, producing a very similar pattern distribution to the control cells incubated at 37 °C (Fig. 2A-D). On the other hand, incubation at 45, 47 and 50 °C produced a progressively stronger and time-dependent reduction of all CI-SCs as well as changes in the proportion and integrity of individual complexes. Thus, only 15 min at 50 °C were sufficient to reduce to around 50% the average level of CI-SCs, while 30 min at this high temperature produced their almost complete disappearance (Fig. 2F and G). In turn, 1 h at 45 and 47 °C reduced CI-SCs to around 35 and 21%, respectively, compared to the control situation at 37 °C (Fig. 2A and F-I, summarized in 2J). The disassembly of CI-SCs was not compensated by the increase in the free form of complex I (CI). Thus, no free CI was detectable in this cell line under any condition indicating that this complex, in the case of the higher temperatures, was rapidly degraded in parallel with SCs disassembly. Free monomeric complex IV (CIV) and complex II (CII) were also significantly reduced in MDA cells at temperatures above 43 °C (Fig. 2C and D, summarized in 2J). On the contrary, although total CIII signal also decreased with heat stress, this was due to its disappearance from CI-SCs since free dimeric CIII ($CIII_2$) as well as $CIII_2$ + IV remained at similar levels or were even increased at 45 and 47 °C (Fig. 2B and J), indicating that these forms arise in part from the disassembled SCs and retain some stability.

An additional incubation of MDA cells for 1 h at 37 °C, after the initial treatment for 1 h at 47 °C, was not sufficient to allow the recovery of RCs and SCs levels (lanes "Rec" in Fig S2) in concordance with the effects on respiration and survival shown in Fig. 1.

The presence, during the incubation, of inhibitors that block OXPHOS activity and hence respiration without compromising cell viability (Fig S3) (1 mM KCN or 1 μM oligomycin) had consequences on RCs and SCs levels that were dependent on the temperature and treatment duration. At 43 and 45 °C after 1 h incubation and at 47 °C after 20 or 40 min, KCN and oligomycin had a small but noticeable effect on SCs (Fig. 2A, B, D and F), partially preserving them. This observation is compatible with the idea that OXPHOS activity does contribute to the SCs de-stabilization by further increasing the temperature in the organelles above the incubation value. However, when the incubation was at 47 °C for 1 h, at 45 °C for 90 min and at 50 °C for 30 min, there was no difference induced by the presence of the inhibitors (Fig. 2A, B and F-I). These results indicate that at higher temperatures and longer incubation times, the de-stabilization effect on SCs is independent of the OXPHOS system activity and of the additional heat that it may produce.

We noticed that, after incubation at 47 °C, abnormal SCs bands migrating below the smaller SC I + III were observed with CIII antibody (Fig. 2B, and Fig. S2C, marked by a red asterisk), revealing an alteration in their composition and most probably reflecting the loss of some subunits normally present in these associations. In addition, a subcomplex evidencing partial degradation of CIV was observed (Fig. 2C, marked by a red asterisk). This abnormal band was also detected after the treatment at 45 °C upon overexposure of the WB and in the IGA assays for CIV (not shown). The appearance of these abnormal bands was not prevented by the presence of inhibitors (Fig. 2B and C).

The quantification of the different bands detected, in 3 independent experiments, after the treatments for 1 h (Fig. 2J) allowed to define three distinct behaviours in response to increasing heat stress: a strong reduction for CI-SCs, a moderate reduction for CIV and CII and no reduction/increase for $CIII_2$. The stronger effect on complex I levels than on the other complexes was confirmed by extraction of total cell proteins after incubation at 45 and 47 °C and detection of specific subunits by WB after SDS-PAGE compared to control cells maintained at 37 °C (Fig S4).

The findings described above for human MDA cells were essentially reproduced in the murine $L929^{Balbc}$ cell line after a similar treatment at high temperatures. Analogous effects of heat stress on morphology and size reduction without detachment from the culture plate, and on viability, were observed for $L929^{Balbc}$ cells. The cell viability was

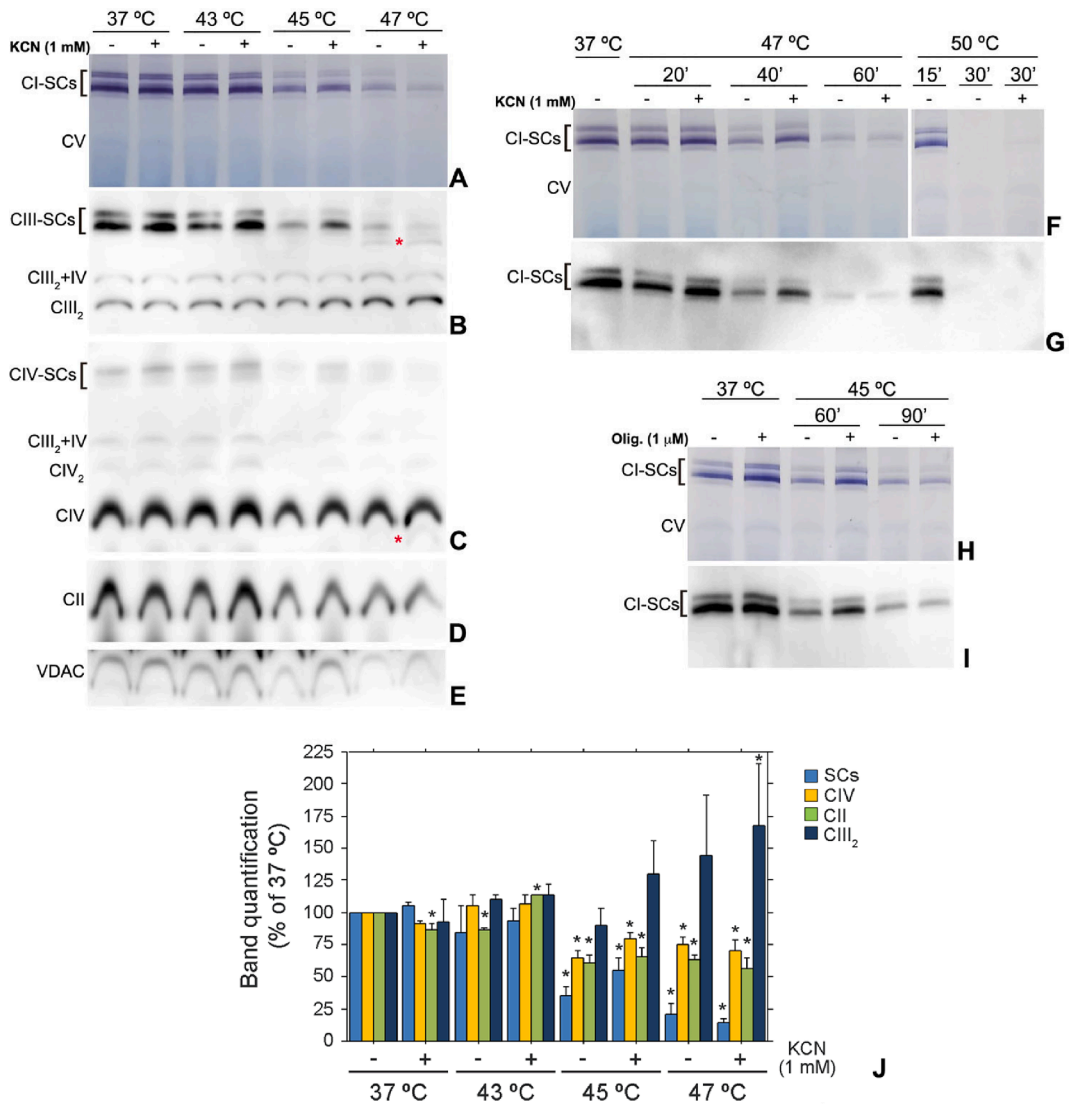

Fig. 2. Effect of high temperatures on mitochondrial complex and SCs stability in human MDA cells. The cells were incubated for 1 h (A-E) or for the indicated times (F-I) at different temperatures in the absence (lanes "-") and in the presence of respiratory inhibitors (1 mM KCN or 1 μM oligomycin ("Olig."); lanes "+") and then the assembly status of RC and SCs was analysed by BN-PAGE followed by IGA or WB detection. A), F) and H) Pattern of complex I-containing supercomplexes (CI-SCs) detected by IGA for NADH dehydrogenase activity. B)-E), G) and I) Immunodetection by western blot of the indicated complex and SCs (antibodies: complex I: NDUFA9; complex III: UQCRC1; complex IV: Cox1; Complex II: SDHA; VDAC complex: porin). The red asterisks in B) and C) indicate abnormal migrating bands detected by anti CIII and anti CIV antibodies, respectively. J) Quantification of the signal obtained by WB for the indicated complex (II, IV and III_2) and by IGA and WB for CI-SCs after incubation at the different temperatures for 1 h in the absence (-) and in the presence (+) of 1 mM KCN (data from 3 independent experiments except for CII (2 experiments), normalization by protein loading; * $p < 0.05$ with respect to 37 °C; see M&M for details). (For interpretation of the references to colour in this figure legend, the reader is referred to the web version of this article.)

progressively reduced with increasing temperature incubation, reaching around 63% compared to 37 °C upon incubation for 1 h at 47 °C, and suffered a further reduction after the 6 h recovery period in the case of the 45 and 47 °C treatments (Fig S5). Concerning the RCs and SCs status, similar quantitative and qualitative effects were also obtained. Thus, incubation at 43 °C for 1 h had a small effect on SCs and complex levels, while incubation at 45 and especially at 47 °C for the same time produced a stronger and differential effect (Fig. 3). The three behaviours previously described for MDA cells were observed again: strong reduction for SCs and for free CI (detectable in this cell line), moderate reduction for free CIV, CV and CII (Fig. 3D, E and F, respectively) and smaller or no reduction for dimeric CIII (Fig. 3C) compared with the controls at 37 °C. These behaviours can be observed in the quantification of the treatment effects on different RCs and on SCs, obtained from two experiments using KCN as inhibitor, shown in Fig. 3H. In this quantification, the levels of CII, CIV and CV were represented together since they showed a very similar trend. The qualitative effect consisting on the appearance of a CIV subcomplex previously described for human cells was also present in this case at 47 °C (Fig. 3D), but the abnormal supercomplexes detected by the CIII antibody were not observed. In the murine cell line, similarly to human cells, the effect of inhibitors (KCN and antimycin A) in preventing SCs de-stabilization was small and especially noticeable at 43 °C, but was not present at 47 °C (Fig. 3A, B and H).

2.3. SCs and CI are unstable at temperatures over 43 °C in liver cells

To analyse these effects in a more physiological setting, liver cells from C57BL/6J (C57) mice were isolated either by the collagenase method (Charni-Natan and Goldstein, 2020) or by a simple mechanical method (see Materials and Methods) and treated at different temperatures as before. Again, a selective time and temperature dependent effect

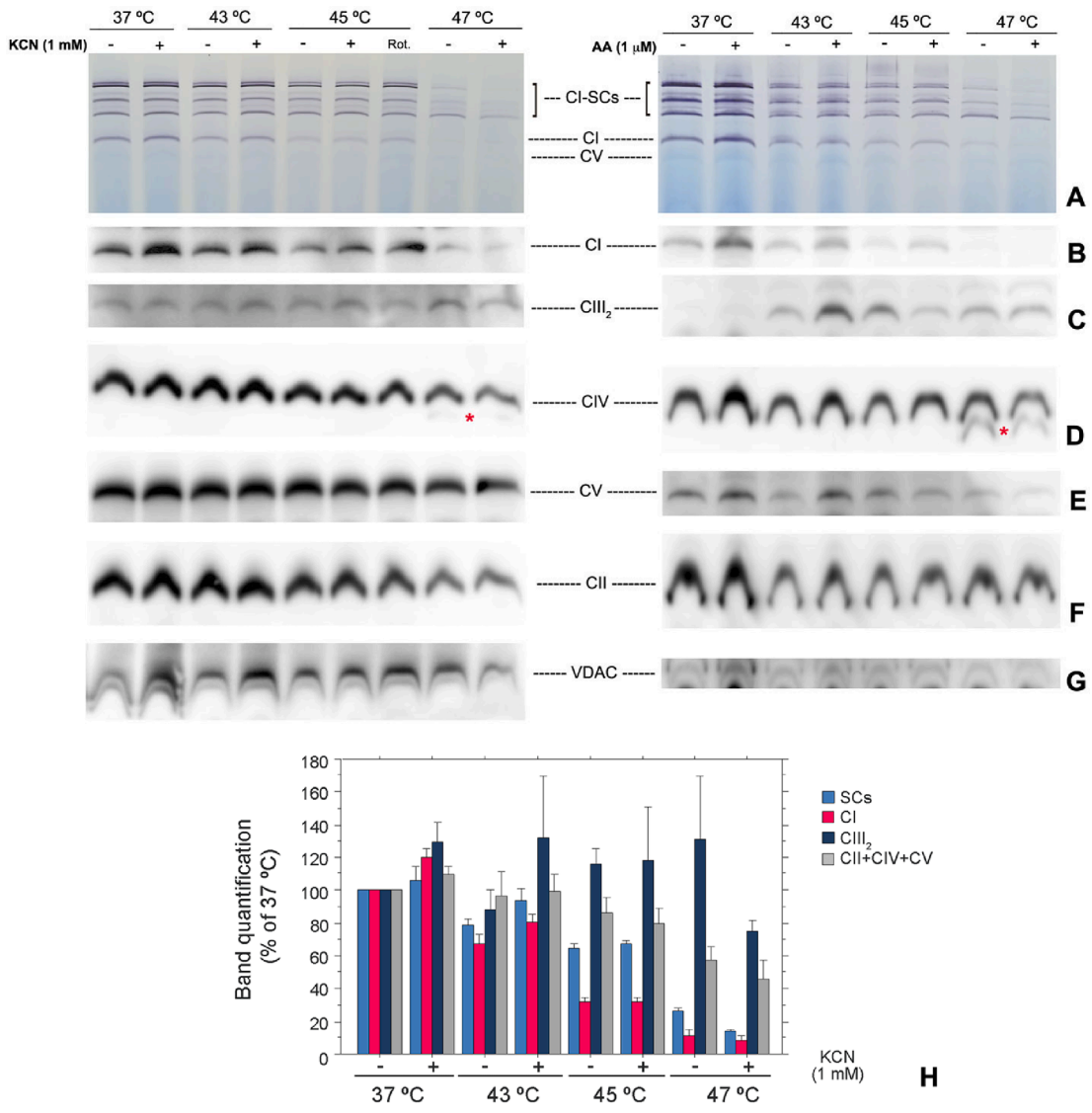

Fig. 3. Effect of temperature on mitochondrial complex and SCs stability in murine L929^{Balbc} cells. The cells were incubated for 1 h at different temperatures in the absence (lanes "-") and in the presence of respiratory inhibitors (lanes "+": 1 mM KCN (left panels) or 1 μM antimycin A ("AA" right panels); lane "Rot.": 1 μM rotenone) and then the assembly status of RC and SCs was analysed as in Fig. 2. A) Pattern of NADH dehydrogenase (complex I) activity detected by IGA. B)-G) Immunodetection by WB of the indicated complex (antibodies: complex I: NDUFA9; complex III: UQCRC1; complex IV: Cox1; Complex II: SDHA; complex V: ATP5F1A; VDAC complex: porin). The red asterisk in D) shows an abnormal migrating band detected by anti-CIV antibody. H) Quantification of the signal obtained by WB for the indicated complex (I, II, IV, V and III_2) and by WB and IGA for CI and CI-SCs after incubation at the different temperatures for 1 h in the absence (-) and in the presence (+) of 1 mM KCN (data from 2 independent experiments; statistical analysis of the differences was omitted; normalization by protein loading). (For interpretation of the references to colour in this figure legend, the reader is referred to the web version of this article.)

on the RCs and SCs pattern was observed with quantitative and qualitative changes (Fig. 4 and Fig S6). The incubation of liver cells at 43 °C for 30 min, produced a mild but consistent reduction of CI-SCs which was paralleled by an increase in free CI levels. Incubation at 45 °C for 30 min produced a stronger disappearance of SCs that was more marked when the treatment at this temperature lasted for 1 h or when it was at 47 °C for 30 min (Fig. 4A-C). Free CI levels increased after incubation at 43 and 45 °C for 30 min compared to controls at 37 °C, but they were reduced after incubation at 45 °C for 1 h and especially at 47 °C for 30 min (Fig. 4A and B). CV and CII suffered a more moderate but also progressive reduction with increasing temperature (Fig. 4E and F), while CIV in its more abundant monomeric form was reduced significantly (Fig. 4D) and generated a subcomplex, that was evident already at 43 °C and increased at 45 and 47 °C (Fig. 4D and Fig S6, panel B, red asterisk), suggesting its partial degradation. In a similar way to what happened in cultured human and murine cells, CIII signal decreased in SCs at the highest temperatures but not in the band corresponding to its free form ($CIII_2$) (Fig. 4C). In summary, liver cells showed the same trend but an even higher sensitivity to heat stress than MDA or L929^{Balbc} cells: incubation for only 30 min at 47 °C produced a similar de-stabilization of SCs in liver cells than did 1 h at the same temperature in cultured cells. Fig. 4H shows the quantification of these effects, obtained from two independent experiments, after 30 min incubation at the different temperatures and in the presence or absence of 1 mM KCN.

In the case of isolated liver cells, the presence of the OXPHOS inhibitor KCN did not show any evident protective effect on respiratory complex and SCs stability at any temperature (Fig. 4 and Fig S6).

2.4. SCs and CI are unstable at temperatures over 43 °C in isolated mitochondria

Isolated mitochondria are a widely used tool to analyse the organelle

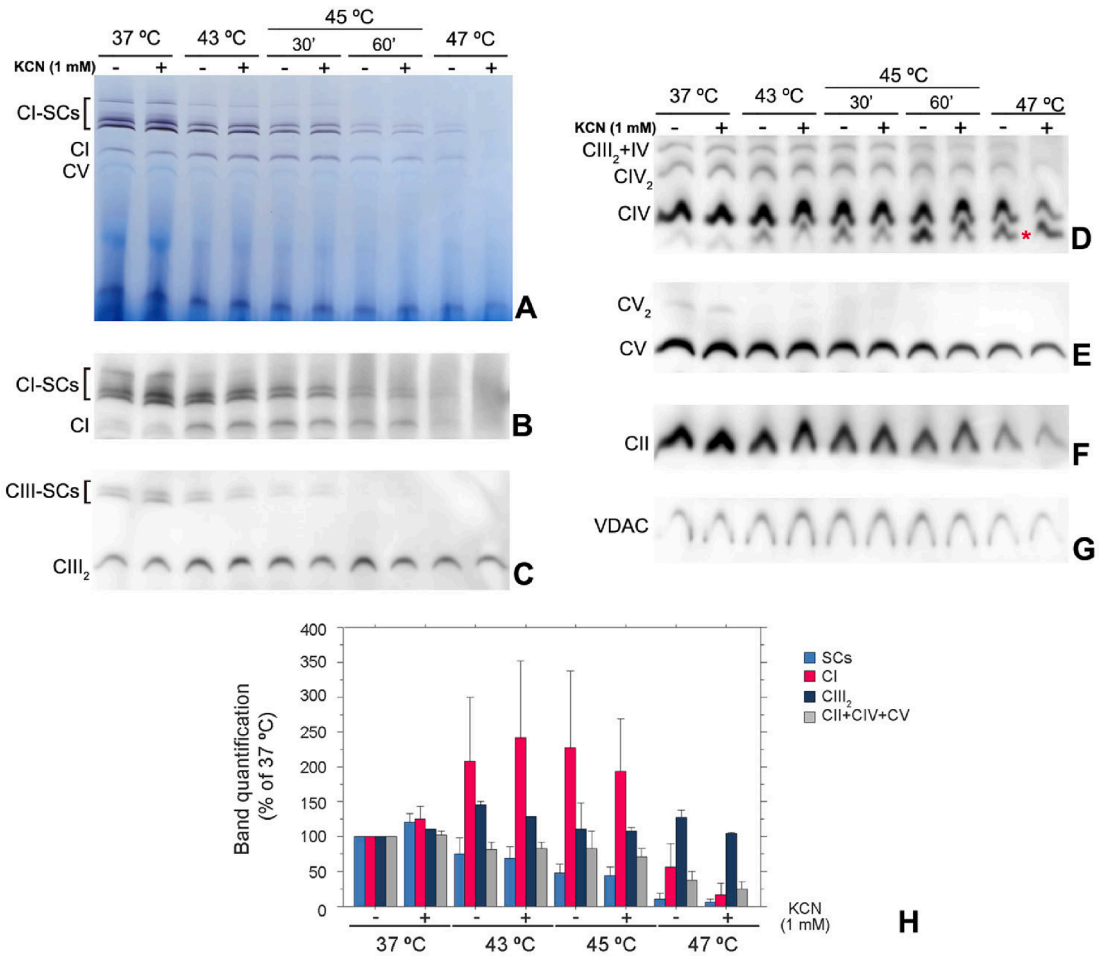

Fig. 4. Effect of temperature on mitochondrial complex and SCs stability in mouse liver cells. The cells, obtained with the collagenase digestion method from animals of the C57BL/6J strain, were incubated at 37, 43 and 47 °C for 30 min and at 45 °C for 30 and 60 min in the absence ("-") and in the presence of 1 mM KCN ("+") and then the RC and SCs assembly status was analysed as before. A) Pattern of CI activity detected by IGA. B)-G) Immunodetection by WB of the indicated complex and SCs (antibodies as in Fig. 3). The red asterisk in D) marks an abnormal migrating band detected by anti-CIV antibody. H) Quantification of the signal obtained by WB for the indicated complex (I, II, IV, V and III_2) and by WB and IGA for CI and CI-SCs after incubation at the different temperatures for 30 min in the absence (-) and in the presence (+) of 1 mM KCN (data from 2 independent experiments; statistical analysis of the differences was omitted; normalized by protein loading). (For interpretation of the references to colour in this figure legend, the reader is referred to the web version of this article.)

functionality that allows easy manipulation while facilitating to discern effects elicited directly on the organelles from those mediated by other cell compartments. We analysed respiration and RCs and SCs stability after incubation at different temperatures in isolated liver mitochondria from C57BL/6J and SWISS mice, two strains showing distinct SCs patterns.

When state 3 respiration was measured in liver mitochondria from C57 mice, incubated for 30 min at 0, 37, 43, 45 and 47 °C, a temperature-dependent progressive drop in the O_2 consumption rate was observed compared with organelles kept at 0 °C (Fig S7). This respiration reduction reached very low values after incubation at 45 and 47 °C: around 22 and 10%, respectively, relative to organelles incubated at 37 °C.

The RCs and SCs pattern in mitochondria from SWISS mice incubated at 37 °C for 30 min was practically identical to that of organelles kept at 0 °C for the same time (Fig. 5). On the contrary, we found that only 15 min at 52 °C, completely de-stabilize SCs and CI while maintaining $CIII_2$ (Fig S8). Lower levels of heat stress had time and temperature-dependent effects similar although not identical to those described before for intact cells and in fact, closer to the ones observed in liver cells. Thus, incubation of isolated liver mitochondria from either SWISS (Fig. 5 and Fig S9 panels A-F) or from C57 mice (Fig S9 panels G and H) at 43–44 °C for 30 min produced a small but noticeable reduction of CI-SCs along with an increase in free CI levels (Fig. 5, left A and B panels; Fig S9A-C). Incubation at 45–46 and especially at 47 °C for 30 min produced a strong disappearance of SCs without further significant increase or even with a decrease of free CI, implying a degradation of this complex (Fig. 5A and B, Fig S9A and C). These effects on CI and SCs were more intense if the treatment was extended to 60 min (Fig. 5, right A and B panels). CV and CII levels were not greatly modified at any temperature (Fig. 5A, E and F, Fig S9B and E), while CIV was moderately and progressively reduced with evidence of its degradation in a smaller subcomplex after incubation at 44 °C and above (Fig. 5D, and Fig S9D, G and H, band indicated by a red asterisk). Free CIII levels ($CIII_2$) as well as those of the association $CIII_2$ + IV, on the contrary, were maintained or even increased at 45 and 47 °C in parallel with SCs disappearance (Fig. 5C and Fig S9B) reproducing again the effects observed in whole cells. The quantification of the bands from the experiments shown in Fig. 5A-F and S9A-F (corresponding to 30 min treatment) is shown in panel 5H, and evidences the differential effects of heat stress previously described.

The inhibition of OXPHOS activity during the incubation, by the presence of KCN, of KCN plus rotenone (Fig. 5, Fig S9G) or by antimycin A (Fig S9G), did not show a protective effect on RCs and SCs levels, and on the contrary, at 45 and 47 °C, it consistently increased the de-stabilization on CI-SCs (Fig. 5 and Fig S9A-C). This effect of KCN on

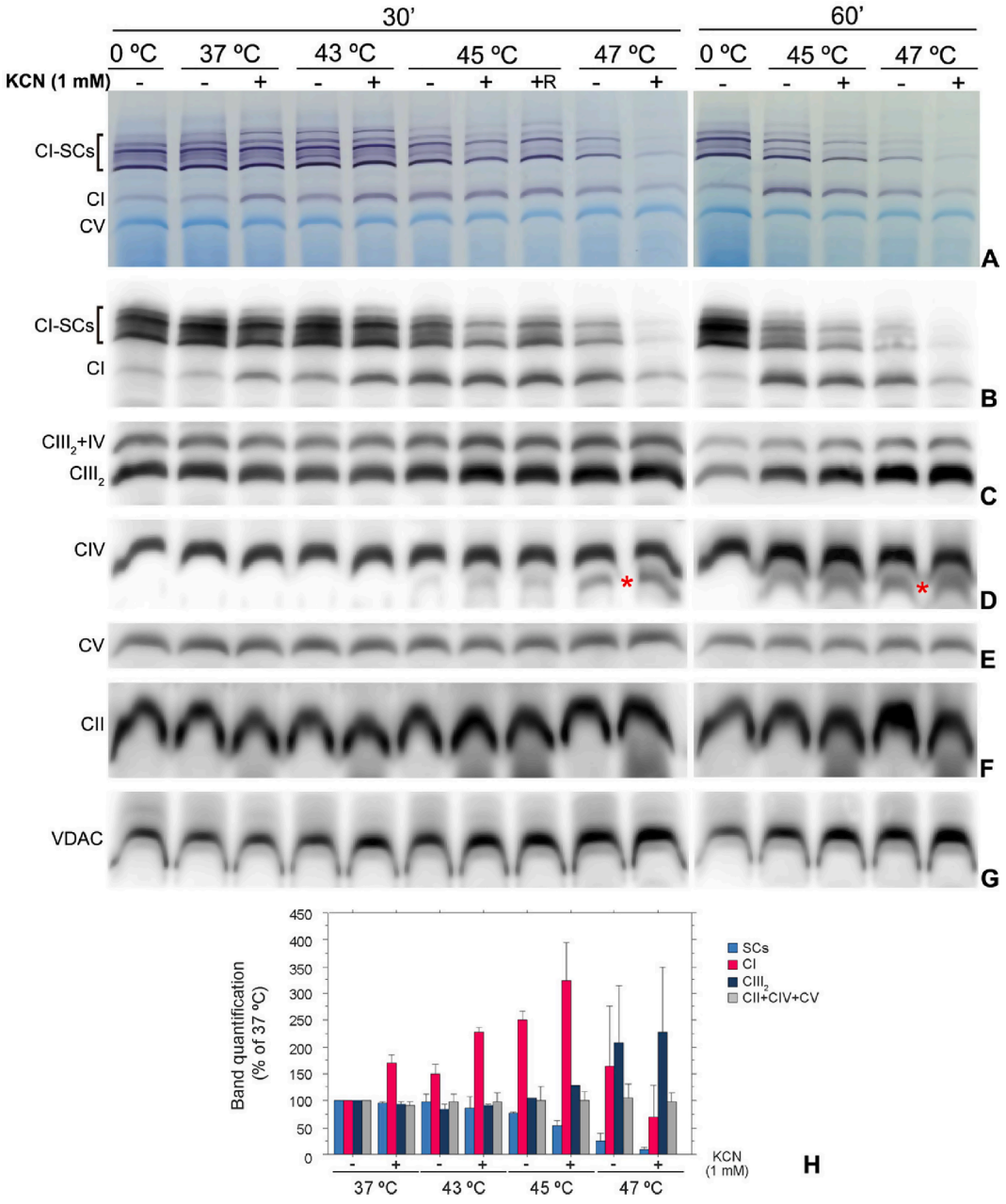

Fig. 5. Effect of temperature on respiratory complex and SCs stability in isolated liver mitochondria. The isolated organelles from mice of the SWISS strain were incubated at 0, 37, 43, 45 and 47 °C for 30 min (left panels) and at 45 and 47 °C for 60 min (right panels) in the absence (lanes "-") and in the presence of 1 mM KCN ("+") or of 1 mM KCN plus 1 μM rotenone ("+R") and then analysed as in previous figures. A) Pattern of CI activity detected by IGA. B)-G) Immunodetection by WB of the indicated complex and SCs (antibodies as in Fig. 4). The red asterisk in D) shows an abnormal migrating band detected by anti-CIV antibody (anti-Cox1). H) Quantification of the signal obtained by WB for the indicated complex (I, II, IV, V and III_2) and by WB and IGA for CI and CI-SCs after incubation at the different temperatures for 30 min in the absence (-) and in the presence (+) of 1 mM KCN (data from 2 experiments; statistical analysis of the differences was omitted; normalized by protein loading). (For interpretation of the references to colour in this figure legend, the reader is referred to the web version of this article.)

CI-SCs was also observed in cultured and liver cells incubated at 47 °C (Figs. 2-4).

In conclusion, although some differences were observed, the main effects of heat stress on RC and SCs stability found in intact liver and cultured cells were reproduced in isolated mitochondria, implying that they are predominantly exerted directly on the organelles and not mediated by other cell compartments.

3. Discussion and conclusions

The proposal that mitochondria work physiologically at around 50 °C in mammalian cells when the respiratory chain is functioning (Chrétien et al., 2018) was surprising because it contradicts previous estimations and theoretical assumptions (Bafou et al., 2014; Hayashi et al., 2015; Homma et al., 2015; Huang et al., 2018; Kiyonaka et al., 2013; Kriszt et al., 2017; Lane, 2018; Macherel et al., 2021; Nakano et al., 2017; Qiao et al., 2018; Savchuk et al., 2019; Fahimi and Matta, 2022). Thus, among the few studies that directly measure temperature in mitochondria, most of them find a smaller gradient with cytoplasm and other compartments, ranging from one to a few degrees [15–22, brilliantly reviewed in 10]. In particular, the publications by Kiyonaka et al. (Kiyonaka et al., 2013) and Nakano et al. (Nakano et al., 2017), both using genetically encoded fluorescent probes directed to mitochondria, report the higher values of temperature in the organelles.

They find an increase in mitochondrial temperature with respect to the incubation value, after inducing uncoupling either with CCCP or FCCP, of around 5 °C in the first case (Kiyonaka et al., 2013) and of 6–9 °C in the other (Nakano et al., 2017). It should be considered, however, that uncoupling promotes maximal OXPHOS activity and that it increases the fraction of chemical energy converted into heat from around 50–60% in state 3 respiration (Nakamura and Matsuoka, 1978; Nath, 2016; Nicholls et al., 2013) to close to 100%, representing hence an extreme and non-physiological situation. In fact, a re-evaluation of the data in (Kiyonaka et al., 2013) by Macherel et al. (Macherel et al., 2021) estimates the mitochondrial temperature in HeLa cells without uncoupling to be around 36–37 °C, the same as the incubation temperature. Other works using different mitochondrial specific sensing probes (both genetic and small molecules), and again after uncoupling to stimulate mitochondrial activity and heat production, report temperatures in mitochondria between 1 and 5 °C higher than the incubation value (Hayashi et al., 2015; Qiao et al., 2018; Savchuk et al., 2019; Homma et al., 2015; Huang et al., 2018; Kriszt et al., 2017; Di et al., 2021).

Thermal physics theoretical estimations (Bafou et al., 2014; Lane, 2018; Macherel et al., 2021; Fahimi and Matta, 2022) also question the possibility of such large temperature gradients inside a cell as those suggested by Chrétien et al. (Chrétien et al., 2018). In addition, concerns regarding the accuracy in temperature sensing of Mito Thermo Yellow (MTY), the thermal probe employed in the mentioned report (Chrétien et al., 2018), have been raised. In particular, MTY response to temperature could be affected by the local environment in confined spaces that are highly packed with proteins such as the mitochondrial matrix or in the vicinity of rotating machines such as the ATP synthase (Lane, 2018; Macherel et al., 2021).

The RCs and SCs pattern, determined by Blue-Native analysis (Wittig and Schägger, 2008; Acín-Pérez et al., 2008; Liang et al., 2022), can reveal differences between cell types and physiological or non-physiological situations, reflecting the cell respiratory capacity (Acín-Pérez et al., 2008; Balsa et al., 2019; Lapuente-Brun et al., 2013; Wittig and Schägger, 2008; Rugolo et al., 2021). We reasoned that, by incubating cells and isolated mitochondria at different temperatures in conditions where OXPHOS function is blocked and cannot contribute to generate heat, and then determining RCs and SCs function and stability, we could obtain information about the maximum physiological values of this parameter that can be reached inside the organelles. Our results show that, after incubation at temperatures up to 42–43 °C, the complex and SCs organization in intact cells and isolated mitochondria, at least during the relatively short times analysed, suffer only minor affectation. Respiratory capacity in cultured cells also seems to be marginally affected after these treatments. On the contrary, incubation at temperatures above 43 °C rapidly and progressively induced the disassembly of SCs and the degradation of some complexes (especially CI and, to a lesser extent, CIV) and severely reduced respiration. The presence of OXPHOS inhibitors had a partial protective effect on RC and SCs stability only at milder heat stress treatments (at temperatures of 43–45 °C and at the shorter times) in cultured cells. This fact suggests that, by preventing a further increase in the applied temperature by the heat generated through mitochondrial activity, the disassembly is slowed down but not completely avoided. When higher temperatures, 47 °C and above, or longer times at 45 °C were applied, the final effect tended to become independent on the presence of inhibitors and hence on the existence of mitochondrial activity. This partially protective effect of different inhibitors (AA for complex III, KCN for complex IV and oligomycin for complex V) was similar in cultured cells but was not observed in the case of liver cells and isolated liver mitochondria which showed a higher sensitivity to heat stress than the established cell lines.

Not all the complexes and SCs were equally sensitive to heat stress. Thus, the largest SCs, all containing complex I (CI-SCs), were more affected by increasing temperature (Figs. 2-5). This differential effect was also evidenced by the fact that CI was massively degraded *in vivo* and *in organello* at the higher temperature values while a good part of free CIV, CV and CII were still preserved (Figs. 2-5). Even more obvious was the different behaviour of CIII, whose proportion in the free dimeric form ($CIII_2$) and associated with CIV ($CIII_2$ + IV) remained constant or even increased at 45 and 47 °C, indicating a higher stability than CI once it is disassembled from the larger SCs (Figs. 2-5). The change in the ratio uncoupled/coupled respiration found after the treatments (from 1.5 in control to around 1.0 in 47 °C-treated cells; Fig. 1C and Fig. S1A) could be explained, at least in part, by the consequences of these heat stress differential effects. Thus, the ratio CV/CI increases dramatically in the treated cells and this could induce a higher use of the remaining OXPHOS capacity, to close to its maximum, in trying to restore the ATP production. This differential sensitivity to temperature, if it is also operating in the physiological range, could represent an additional factor in the regulation of RCs and SCs assembly and organization.

The results obtained in the *in organello* experiments, reproducing the main features of RCs and SCs disassembly and degradation observed in intact cells, allow to exclude that these effects elicited by heat stress could be mediated by other compartments and due, for example, to increased mitophagy. They strongly point, instead, at a direct mitochondrial mechanism. This conclusion is also supported by the very short time required to observe the effects (after only 15–20 min at the higher temperatures, Fig. 2F and G and Fig S8) and by the differential consequences on individual RC and SCs discussed above.

SCs in cultured cells showed higher resistance to heat stress than in liver cells or in isolated liver mitochondria (independently of the mouse strain), since 30 min at 47 °C had a similar or higher effect on their stability in liver cells than 1 h at the same temperature in MDA and $L929^{Balbc}$ cells (Figs. 2 and 3 vs Fig. 4). In the same direction, a CIV degradation band (indicating complex damage) was also more evident in liver cells and in isolated liver mitochondria at shorter times and lower temperatures than in cultured cells. These facts could be related to the adaptation of cultured cells to grow under conditions of high oxygen and increased basal reactive oxygen species (ROS) production (Halliwell, 2014; Jagannathan et al., 2016), to the faster turnover of organelles associated with rapid growth in culture, to the lipid composition differences or even to mitochondrial structural or metabolic differences among the various cell types.

Our observations agree with previous studies showing that heat stress above 43 °C negatively affects mitochondrial function and structure causing mitochondrial membrane depolarization and an increase in ROS generation (Feng et al., 2019; Roti Roti, 2008; Zhao et al., 2006; Zukiene et al., 2010) as well as increased proton leak associated with disorganization in the inner membrane lipid bilayer (Willis et al., 2000). Morphological consequences of heat stress include cristae reduction, swelling and membrane disruption (Qian et al., 2004) or increase in organelle fission (Yu et al., 2018). Those effects are associated to decreased ATP production and protein stability disruption (Wilkening et al., 2018) and finally contribute to apoptosis (Qian et al., 2004; Roti Roti, 2008; Zhao et al., 2006; Žūkienė et al., 2017). These alterations in mitochondrial activity and structure have been shown to be time and temperature dependent (Feng et al., 2019; Roti Roti, 2008; Willis et al., 2000; Yu et al., 2018; Zukiene et al., 2010; Žūkienė et al., 2017; Wilkening et al., 2018) with tissue, age and even gender specific differences (Naučienė et al., 2012; Šilkūnienė et al., 2018).

Although they remain to be investigated, different molecular mechanisms, alone or in combination, could explain the observed effects on RCs and SCs stability. These include from mainly physical effects induced by heat stress on protein folding and on protein-lipids interactions (Roti Roti, 2008; Willis et al., 2000) or the increase in ROS generation (Chen and Zweier, 2014; Feng et al., 2019; Pryde et al., 2016; Roti Roti, 2008; Zukiene et al., 2010; Kang et al., 2018) to the activation of mitochondrial proteases (Augustin et al., 2005; Deng et al., 1998; Patron et al., 2022; Zurawa-Janicka et al., 2013).

The determination of the mitochondrial temperature physiological range is important to understand the heat generation and maintenance mechanisms, and has implications in pathology. Thus, both the

susceptibility to high temperature damage as well as the response to hyperthermia as a therapeutic approach could depend on variations in heat generation and tolerance by mitochondria (Lane, 2018). In this respect, it will be interesting to analyse possible differences among mitochondrial haplotypes as well as among tissues and metabolic situations in heat generation and in the response to heat stress. In fact, the different survival rate after sepsis observed between human individuals with the H and other haplotypes has been associated to a possible different heat generation capacity of their mitochondria (Baudouin et al., 2006). In the same direction, the potential effects of uncouplers, that would be expected to increase heat production as well as the effects of lower, more "physiological" temperatures (in the 40–43 °C range), and longer treatment times deserve also a detailed study.

From our results, the SCs de-stabilization appears to be an early and direct effect of heat stress in mitochondria, and we also observe that the recovery of SCs levels after the heat stress has been removed, if possible, is not a rapid phenomenon (Fig 1 and S3 Fig). Some of the negative consequences observed after prolonged fever such as fatigue or loss of OXPHOS capacity (Francoeur, 2015; Ames et al., 2017) could be related to these facts.

Our findings cannot exclude that high temperatures may be reached inside mitochondria at certain points or during short times (Fahimi and Matta, 2022), but they are clearly in contradiction with the idea that mitochondria as a whole, and more precisely the OXPHOS system, can operate and have its optimum function at close to 50 °C (Chrétien et al., 2018). In contrast, our results indicate that, even in the absence of substantial OXPHOS activity contribution to heat production, the SCs are unstable above 43 °C, strongly suggesting that optimal mitochondrial function is incompatible with maintained higher temperatures in the organelles.

4. Materials and methods

4.1. Animals

Mice were housed at the animal facility under strictly controlled, specific-pathogen-free conditions. Animals were maintained with a rodent diet (2914 Teklad Global 14% protein rodent maintenance diet) and water was made available *ad libitum* in a vivarium with a 12-h light–dark cycle at 22 °C. Experiments were performed in accordance with ethical guidelines and international standards and with the approval of the ethical committee (protocol n°: PI38/21). Between 2 and 4 female mice of the indicated strains (either C57BL/6JOlaHsd (referred to as "C57" or "C57BL/6J") or RjOri:SWISS (referred to as "SWISS"), 2 to 6 months old, were used per experiment.

4.2. Liver cell preparation and treatments

Liver cells were obtained by two different procedures:

a) The collagenase digestion method essentially as described in (Charni-Natan and Goldstein, 2020), except that the last purification step involving Percoll gradients was omitted.
b) A simple mechanical method intended to accelerate the isolation of cells and to prevent treatments that could interfere with mitochondrial activities. Briefly, the livers were removed after sacrifice and placed in cold medium A (10 mM Tris-HCl, pH 7.4, 0.32 M sucrose, 1 mM EDTA, 5 mM $MgCl_2$), then they were finely chopped with scissors and washed several times with cold medium A to remove blood and cell debris. Next, the liver small pieces were transferred to a glass homogenizer and disaggregated in medium A (10 ml/g of tissue) containing 2 mg/ml BSA and a protease inhibitor cocktail (cOmplete ™ Protease Inhibitor Cocktail (Roche)), using a loose-fitting pestle (0.1 mm clearance) rotating at 300 rpm, with just one up and down passage. The cell suspension was filtered through three layers of gauze and cells and small cell clumps were collected by centrifugation at 500 × g/2 min, resuspended and washed twice in the same way to eliminate blood and cell debris. After the last centrifugation, the cells were resuspended in 10 ml of DMEM medium and were counted. Viability was around 80% by trypan blue exclusion determination. The time from sacrifice to starting of the incubation with this procedure was around 35 min.

After counting, the liver cells were diluted to approx. $3x10^5$ cells/ml in DMEM containing 10% FBS and 5 mM glucose and, for each treatment condition, a volume of 5–7 ml of this suspension was placed in a 50 ml corning tube and incubated, with the lids open to allow gas exchange, at the desired temperature in a regular cell culture incubator with 5% CO_2, either in the presence or absence of complex IV inhibitor KCN at 1 mM final concentration. After the treatment, the tubes were cooled in an ice bath, the cells were collected by centrifugation and homogenized to obtain isolated mitochondria as described (Fernández-Vizarra et al., 2010).

Five independent experiments were performed with freshly isolated hepatocytes in all cases from C57 mice (2 animals/experiment). In three of them the mechanical isolation method was used and incubation was for 30 min with 45 °C as the maximum temperature reached (one such experiment is shown in figure S6) and two experiments were performed using the collagenase method and reaching 47 °C (one is shown in Fig. 4A-G and both are quantified in panel 4H). No big differences were found in the effects of temperature on RCs ad SCs stability among cells obtained by both methods (see Fig. 4 for the collagenase method and Fig. S6 for the mechanical method results).

4.3. Cell culture and treatments

The human MDA-MB468 breast cancer and the mouse $L929^{Balbc}$ cell lines were cultured in high glucose DMEM (GIBCO™) medium supplemented with 10% FBS (GIBCO™) and with penicillin/streptomycin (GIBCO™). The $L929^{Balbc}$ cell line was obtained in our laboratory by transferring mitochondria from platelets of mouse strain BALB/cJ, to an L929 derivative mtDNA-less cell line (ρ°L929neo) (Acín-Pérez et al., 2003). The cells were counted and seeded the day before in order to have the appropriate density (80–90% coverage) at the time of treatment, and around 1.5 $x10^7$ cells were used per treatment condition.

To analyse the effect of temperature on RC and SC stability in whole cells, fresh medium with or without OXPHOS inhibitors (KCN, oligomycin, antimycin A or rotenone) at concentrations that block mitochondrial respiration without affecting cell viability (1 mM for KCN and 1 μM for the rest, see Fig S3) was pre-heated and added to the cells at 3–5 °C below the target temperature, in order to reduce the time to reach the desired value. The temperature inside control plates, measured with a thermocouple thermometer after 10–20 min of incubation, showed values ±0.3 °C around the selected value in the incubator.

After the treatment, the cells were cooled down to RT, collected by trypsinization, centrifuged and processed to obtain mitochondrial lysates and to analyze the RCs and SCs status by Blue Native PAGE as described (Wittig and Schägger, 2008; Acín-Pérez et al., 2008). Briefly, cells (approx. 1.5 $x10^7$) were collected after trypsinization and washed twice with cold PBS. Cell pellets were frozen at –80 °C to increase cell breakage and were homogenized in a tightly fitting glass-teflon homogenizer with about 10 cell pellet volumes of homogenizing buffer A (83 mM sucrose, 10 mM MOPS, pH 7.2). After adding an equal volume of buffer B (250 mM sucrose, 30 mM MOPS, pH 7.2), nuclei and unbroken cells were removed by centrifugation at 1000 *g* during 5 min. Mitochondria were collected from the supernatant by centrifuging at 12,000 *g* during 2 min and washed once under the same conditions with buffer C (320 mM sucrose, EDTA 1 mM, 10 mM Tris-HCl, pH 7.4). Protein concentration was determined using the Bradford method (Bradford, 1976) and the mitochondrial pellets were suspended in an appropriate volume of buffer D to be at 10 mg/ml (50 mM NaCl, 50 mM imidazole/HCl, 2 mM 6-aminohexanoic acid, 1 mM EDTA, pH 7.0).

No differences in the proportion of detached cells were observed among the various treatments. However, the treatment at 47 °C consistently reduced the yield of final mitochondrial protein with respect to the control at 37 °C by about 30%. The amount of protein of the different treatments loaded on the blue native gels was equalized to allow normalization (see below).

Seven experiments were performed with MDA cells using different conditions (temperatures, times and inhibitors). The results shown in Fig. 2 correspond to one representative experiment (out of three) using KCN and one with oligomycin. Four experiments were performed with $L929^{Balbc}$ cells: two with KCN under identical conditions (one of them shown in Fig. 3A-G left panels and both used for the quantification in Fig. 3H) and one with antimycin A (shown in Fig. 3A-G right panels).

4.4. Cell viability assays

Cell viability was determined by the trypan blue exclusion test (Strober, 2001). Cells were collected by trypsinization, resuspended in PBS and mixed with an equal volume of 0.4 % trypan blue (Sigma) in 15 mM NaCl and live and dead cells were counted using a hemocytometer.

4.5. Cell death assays

For the measurement of cell death induction, cells were stained for 15 min at room temperature with a mixture of Annexin-V-FITC (Immunostep), which binds to the phosphatidylserine exposed in the cell surface, and 7-AAD (7-aminoactinomycin, Biolegend), which binds DNA and changes its absorbance, indicating cell damage, in annexin-binding buffer (140 mM NaCl, 2.5 mM $CaCl_2$, 10 mM HEPES/NaOH, pH 7.4). Then they were washed twice with PBS and collected by centrifugation. Finally, they were resuspended in 200 µl of cold PBS for assessment in a FACSCalibur (BD Biosciences) cytometer (Marco-Brualla et al., 2019). Data from the cytometer were analysed using the FlowJo software.

4.6. Mitochondrial isolation and incubations

Mitochondrial fractions for *in organello* experiments were isolated from mouse liver as previously described (Fernández-Vizarra et al., 2010). Equal amounts of the final mitochondrial suspension (typically 0.4–0.5 ml at a protein concentration of approx. 1 mg/ml) were distributed in 1.5 ml Eppendorf tubes and placed at the desired temperatures in heating blocks with gently shaking to avoid sedimentation of the organelles. Incubation medium contained: 25 mM sucrose, 75 mM sorbitol, 100 mM KCl, 0.05 mM EDTA, 5 mM $MgCl_2$, 10 mM Tris–HCl, pH 7.4, and 10 mM H_3PO_4 and the final pH of the solution was adjusted to 7.4 with 0.5 M Tris base. 2 mg/ml fatty acid-free BSA, 1 mM ADP, 10 mM glutamate, and 2.5 mM malate were added to the medium to support mitochondrial respiratory activity. When corresponding, specific OXPHOS inhibitors (KCN, rotenone or antimycin A) were added from a 100X stock solution to the corresponding tubes before starting the incubation. After the treatments, the tubes were cooled on ice and the mitochondria were collected by centrifugation and treated for BN-PAGE analysis as described below.

Six experiments were performed with liver isolated mitochondria using different conditions (temperatures, times and inhibitors): four from C57BL/6J mice and two from SWISS mice (3 to 4 animals/experiment in all cases). Representative examples of the results are shown in figures 5, S8 and S9.

4.7. Respiration measurements

O_2 consumption in intact cells was determined with an oxytherm Clark-type electrode (Hansatech) as previously described (Hofhaus et al., 1996) with small modifications (Acín-Pérez et al., 2003). Respiratory activity in isolated mitochondria was measured as previously described (Fernández-Vizarra et al., 2010). Additional information on coupling degree was obtained in intact cells after incubation at 37, 45 and 47 °C by respiration measurement in the presence of titrated quantities of oligomycin. Briefly, after registering basal respiration, small amounts of oligomycin were added to the oxygen electrode chamber using a Hamilton syringe until maximal inhibition of oxygen consumption (that happened to be ~ 20% of basal respiration rate in all three cases analyzed) was reached. Then, the uncoupler DNP was added (at a final concentration of 65 µM) to evaluate the maximal respiratory capacity of cells. Finally, respiration was inhibited with KCN at 4 mM.

4.8. Blue Native polyacrylamide electrophoresis

Mitochondrial fractions obtained from cultured cells or liver cells after the treatments of intact cells, as well as the isolated liver mitochondria after the *in organello* experiments were processed for BN-PAGE analysis to determine their RC and SCs levels and assembly status. First, the protein concentration in the mitochondrial preparations was determined, they were resuspended at 10 mg/ml and digitonin (from a 10% stock) was added to a final concentration of 4 mg detergent/mg of protein (Wittig and Schägger, 2008). After centrifugation at full speed (14 Krpm) in a microcentrifuge for 30 min to remove insoluble material, digitonin-solubilized mitochondrial proteins (50–80 µg for IGA and 30–50 µg for WB) were separated on blue native gradient gels (3–13% acrylamide, Novex). After electrophoresis, the gels were further processed for WB or for in gel complex I and/or complex IV activity (IGA) as described (Acín-Pérez et al., 2008). In some cases, after the IGA assay, the gels were fixed with methanol/acetic acid and stained with Coomassie blue.

4.9. Analysis of mitochondrial RC and SCs status by Western-blot

After BN-PAGE, the proteins were electroblotted onto PVDF membranes, and then the membranes were blocked with PBS-T buffer containing 5% non-fat milk. Antibodies (in PBS-T containing 0.5% non-fat milk) against complex I, anti-NDUFA9 (Invitrogen); complex III, anti-Uqcrc1 (Invitrogen); complex IV, anti-COI (Invitrogen); complex II, anti-SDHA (Novex-Life Technologies); complex V, anti-α-F_1-ATPase (Mitosciences); and VDAC, anti-porin (Abcam), were used to incubate the membranes. In some experiments antibodies for different complexes were incubated and detected simultaneously on the same blot. After that, membranes were washed again with PBS-T and incubated with 0.2 µg/ml of the secondary antibody labelled with peroxidase (Sigma). Finally, proteins were revealed with the Pierce ECL Western Blotting Substrate (Thermo Scientific). The signal was documented using the Amersham Imager 600 and quantified with the instrument included application.

Complementary analysis of the temperature treatment effects on RCs subunits steady state was performed by SDS-PAGE electrophoresis of total cell proteins from MDA and $L929^{Balbc}$ cells. After the different incubations (at 37, 45 and 47 °C for 1 h), the cells were collected from 60 mm-diameter culture plates, washed twice with PBS and total proteins were extracted using RIPA buffer containing protease inhibitors. Around 20 µg of total protein from each treatment were run in a 12.5% acrylamide/bisacrylamide SDS-PAGE and electroblotted onto PVDF membranes which were probed with specific antibodies to detect different RCs subunits and porin.

4.10. In gel complex I and complex IV activity assay (IGA assay)

For the determination of in gel complex I activity after electrophoresis (IGA for CI), the polyacrylamide gel was submerged in a solution of Tris-HCl 5 mM, pH 7.4, NADH 0.1 mg/ml and Nitro tetrazolium Blue chloride (NBT) 2.5 mg/ml. Complex I activity is revealed by a dark-blue precipitate forming in the corresponding bands that appears between 10 and 30 min but continues to develop for several hours. Complex V is

usually visible in the blue native gels as a light blue band because it is very abundant and binds the Coomassie brilliant blue G-250 that is present in the sample loading and running buffers (Wittig and Schägger, 2008).

For cytochrome *c* oxidase activity detection (IGA for CIV), the gel was incubated with 50 mM Potassium Phosphate buffer; pH 7.2; containing 0.05% diaminobenzidine (DAB) and 50 μM reduced cytochrome *c*. Complex IV activity is revealed as a brown precipitate in the corresponding bands that appears typically between 30 and 60 min but continues to develop for several hours.

The gels were placed on a white translucid screen (BioRad)) and photographed with a digital camera at a distance of around 15 cm (against natural light). The signal corresponding to CI (or CIV) activity was quantified on the picture by densitometry, in a similar way to WB assays, using the Image J analysis software (Rasband, W.S., ImageJ, U. S. National Institutes of Health, Bethesda, Maryland, USA.). The results obtained for CI-SCs with the IGA and WB assays were very coincident (see, for example, Fig. 2A and 2B or 2E-H) and were combined for the quantification shown in Fig. 2I. In the case of CIV, some discrepancies were found in some cases between the signal obtained by the IGA assay and that of the WB, and thus only the data from the latter were used for quantification of this complex.

Note: The pattern of RC and SCs observed by IGA or WB after Blue Native electrophoresis (the bands observed and their proportions) shows differences depending on the species, strain, the cell type and the physiological or pathological situation (for a characterization see references 28–33 and therein). All the SCs migrating above isolated CI (which has a molecular mass of about 1 MDa) contain CI and CIII and only some of them contain also CIV. The relationship among the different SCs forms and their precise role in respiration are still under investigation. Although the effects of high temperatures described in this work were not exactly the same on all the bands corresponding to these SCs, they have been considered together for simplicity.

4.11. Statistics

Results, displayed as mean ± SEM, were statistically analysed by ANOVA using the statistical package Stat View 5.0 (SAS Institute). Statistically significant p values were indicated: * $p \leq 0.05$.

Chemicals and reagents were purchased from Sigma-Aldrich except where otherwise noted.

Funding

This work was supported by grant number “PGC2018-095795-B-I00” from Ministerio de Ciencia e Innovación (https://ciencia.sede.gob.es/) to PF-S and RM-L, and by grants “Grupo de Referencia: E35_17R” and grant number “LMP220_21” to P.F.-S. and R.M.-L. from Diputación General de Aragón (DGA) (https://www.aragon.es/). The work of RSA was supported by a grant from the Spanish Association Against Cancer in Aragón (PRDAR21487SOLE).

Declaration of Competing Interest

The authors declare that they have no known competing financial interests or personal relationships that could have appeared to influence the work reported in this paper.

Acknowledgements

Authors would like to acknowledge the use of Servicio General de Apoyo a la Investigación-SAI, Universidad de Zaragoza. We also would like to thank Dr. Chantal Reina-Ortiz for proofreading the manuscript. We thank the Spanish Ministerio de Ciencia e Innovación (Grant “PGC2018-095795-B-I00”), Diputación General da Aragón (Grants “Grupo de Referncia E35-17R” and “LMP220_21”) and the Spanish Association Against Cancer in Aragón (Grant "PRDAR21487SOLE") for financial support.

Appendix A. Supplementary data

Supplementary data to this article can be found online at https://doi.org/10.1016/j.mito.2023.02.002.

References

Acín-Pérez, R., Bayona-Bafaluy, M.P., Bueno, M., et al., 2003. An intragenic suppressor in the cytochrome c oxidase I gene of mouse mitochondrial DNA. Hum. Mol. Genet. 12 (3), 329–339. https://doi.org/10.1093/hmg/ddg021.

Acín-Pérez, R., Fernández-Silva, P., Peleato, M.L., Pérez-Martos, A., Enriquez, J.A., 2008. Respiratory active mitochondrial supercomplexes. Mol. Cell 32 (4), 529–539. https://doi.org/10.1016/j.molcel.2008.10.021.

Ames, N.J., Powers, J.H., Ranucci, A., Gartrell, K., Yang, L., VanRaden, M., et al., 2017. A systematic approach for studying the signs and symptoms of fever in adult patients: the fever assessment tool (FAST). Health Qual. Life Outcomes 15 (1), 84. https://doi.org/10.1186/s12955-017-0644-6. PMID: 28449675; PMCID: PMC5408372.

Augustin, S., Nolden, M., Müller, S., Hardt, O., Arnold, I., Langer, T., 2005. Characterization of peptides released from mitochondria: evidence for constant proteolysis and peptide efflux. J. Biol. Chem. 280 (4), 2691–2699. https://doi.org/10.1074/jbc.M410609200. Epub 2004 Nov 19 PMID: 15556950.

Bafou, G., Rigneault, H., Marguet, D., Jullien, L., 2014. A critique of methods for temperature imaging in single cells. Nat. Methods 11, 899±901. https://doi.org/10.1038/nmeth.3073. PMID: 25166869.

Balsa, E., Soustek, M.S., Thomas, A., et al., 2019. ER and Nutrient Stress Promote Assembly of Respiratory Chain Supercomplexes through the PERK-eIF2α Axis. Mol. Cell 74 (5), 877–890.e6. https://doi.org/10.1016/j.molcel.2019.03.031.

Baudouin, S.V., Saunders, D., Tiangyou, W., et al., 2006. Mitochondrial DNA and survival after sepsis: a prospective study [published correction appears in Lancet. 367(9524), 1730]. Lancet. 2005;366(9503):2118-2121. doi:10.1016/S0140-6736(05)67890-7.

Bradford, M.M., 1976. A rapid and sensitive method for the quantitation of microgram quantities of protein utilizing the principle of protein-dye binding. Anal. Biochem. 72, 248–254.

Charni-Natan, M., Goldstein, I., 2020. Protocol for Primary Mouse Hepatocyte Isolation. STAR Protoc. 1 (2), 100086 https://doi.org/10.1016/j.xpro.2020.100086.

Chen, Y.R., Zweier, J.L., 2014. Cardiac mitochondria and reactive oxygen species generation. Circ. Res. 114 (3), 524–537. https://doi.org/10.1161/CIRCRESAHA.114.300559. PMID: 24481843; PMCID: PMC4118662.

Chrétien, D., Bénit, P., Ha, H.-H., Keipert, S., El-Khoury, R., Chang, Y.-T., et al., 2018. Mitochondria are physiologically maintained at close to 50 °C. PLoS Biol 16 (1), e2003992. https://doi.org/10.1371/journal.pbio.2003992.

Clarke, A., 2017. Principles of Thermal Ecology: Temperature. Energy and Life. OUP, Oxford, UK. https://doi.org/10.1093/oso/9780199551668.001.0001.

Clarke, A., Pörtner, H.O., 2010. Temperature, metabolic power and the evolution of endothermy. Biol. Rev. 85, 703–727. https://doi.org/10.1111/j.1469-185X.2010.00122.x. PMID: 20105154.

Deng, K., Zhang, L., Kachurin, A.M., Yu, L., Xia, D., Kim, H., Deisenhofer, J., Yu, C.A., 1998. Activation of a matrix processing peptidase from the crystalline cytochrome bc1 complex of bovine heart mitochondria. J. Biol. Chem. 273 (33), 20752–20757. https://doi.org/10.1074/jbc.273.33.20752. PMID: 9694818.

Di, X., Wang, D., Zhou, J., et al., 2021. Quantitatively Monitoring *In Situ* Mitochondrial Thermal Dynamics by Upconversion Nanoparticles. Nano Lett. 21 (4), 1651–1658. https://doi.org/10.1021/acs.nanolett.0c04281.

Feng, Q.W., Cui, Z.G., Jin, Y.J., Sun, L., Li, M.L., Zakki, S.A., et al., 2019. Protective effect of dihydromyricetin on hyperthermia-induced apoptosis in human myelomonocytic lymphoma cells. Apoptosis 24 (3–4), 290–300. https://doi.org/10.1007/s10495-019-01518-y. PMID: 30684145.

Fernández-Vizarra, E., Ferrín, G., Pérez-Martos, A., Fernández-Silva, P., Zeviani, M., Enríquez, J.A., 2010. Isolation of mitochondria for biogenetical studies: An update. Mitochondrion 10, 253–262. https://doi.org/10.1016/j.mito.2009.12.148.

Francoeur, R.B., 2015. Using an innovative multiple regression procedure in a cancer population (Part II): fever, depressive affect, and mobility problems clarify an influential symptom pair (pain–fatigue/weakness) and cluster (pain–fatigue/weakness–sleep problems). Onco Targets Ther. 8, 57–72. https://doi.org/10.2147/OTT.S68859.

Halliwell, B., 2014. Cell culture, oxidative stress, and antioxidants: avoiding pitfalls. Biomed J. 37 (3), 99–105. https://doi.org/10.4103/2319-4170.128725.

Hayashi, T., Fukuda, N., Uchiyama, S., Inada, N., 2015. A cell-permeable fluorescent polymeric thermometer for intracellular temperature mapping in mammalian cell lines. PLoS One 10 (2), e0117677.

Hofhaus, G., Shakeley, R.M., Attardi, G., 1996. Use of polarography to detect respiration defects in cell cultures. Methods Enzymol. 264, 476–483. https://doi.org/10.1016/s0076-6879(96)64043-9.

Homma, M., Takei, Y., Murata, A., Inoue, T., Takeoka, S., 2015. A ratiometric fluorescent molecular probe for visualization of mitochondrial temperature in living cells. Chem. Commun. 51, 6194–6197. https://doi.org/10.1039/C4CC10349A.

Huang, Z., Li, N., Zhang, X., Wang, C., Xiao, Y., 2018. Fixable molecular thermometer for real-time visualization and quantification of mitochondrial temperature. Anal. Chem. 90, 13953–13959. https://doi.org/10.1021/acs.analchem.8b03395.

Fahimi, P., Matta, C.F., 2022. The hot mitochondrion paradox: reconciling theory and experiment. Trends in Chemistry 4 (2), 96–102. https://doi.org/10.1016/j.trechm.2021.10.005.

Jagannathan, L., Cuddapah, S., Costa, M., 2016. Oxidative stress under ambient and physiological oxygen tension in tissue culture. Curr Pharmacol Rep. 2(2), 64-72. doi: 10.1007/s40495-016-0050-5. Epub 2016 Jan 23. PMID: 27034917; PMCID: PMC4809260.

Kang, P.T., Chen, C.L., Lin, P., Zhang, L., Zweier, J.L., Chen, Y.R., 2018. Mitochondrial complex I in the post-ischemic heart: reperfusion-mediated oxidative injury and protein cysteine sulfonation. J. Mol. Cell Cardiol. 121, 190-204. doi: 10.1016/j.yjmcc.2018.07.244. Epub 2018 Jul 20. PMID: 30031815; PMCID: PMC6103816.

Kiyonaka, S., Kajimoto, T., Sakaguchi, R., Shinmi, D., Omatsu-Kanbe, M., Matsuura, H., et al., 2013. Genetically encoded fluorescent thermosensors visualize subcellular thermoregulation in living cells. Nat. Methods 10 (12), 1232–1238. https://doi.org/10.1038/nmeth.2690.

Kriszt, R., Arai, S., Itoh, H., Lee, M.H., Goralczyk, A.G., Ang, X.M., et al., 2017. Optical visualisation of thermogenesis in stimulated single cell brown adipocytes. Sci. Rep. 7 (1), 1383. https://doi.org/10.1038/s41598-017-00291-9.

Lane, N., 2018. Hot mitochondria? PLoS Biol 16 (1), e2005113. https://doi.org/10.1371/journal.pbio.2005113.

Lapuente-Brun, E., Moreno-Loshuertos, R., Acín-Pérez, R., et al., 2013. Supercomplex assembly determines electron flux in the mitochondrial electron transport chain. Science 340 (6140), 1567–1570. https://doi.org/10.1126/science.1230381.

Liang, T., Deng, J., Nayak, B., Zou, X., Ikeno, Y., Bai, Y., 2022. Characterizing the Electron Transport Chain: Structural Approach. Methods Mol. Biol. 2497, 107–115. https://doi.org/10.1007/978-1-0716-2309-1_7.

Macherel, D., Haraux, F., Guillou, H., Bourgeois, O., 2021. The conundrum of hot mitochondria. Biochim. Biophys. Acta Bioenerg. 1862 (2), 148348 https://doi.org/10.1016/j.bbabio.2020.148348.

Marco-Brualla, J., Al-Wasaby, S., Soler, R., et al., 2019. Mutations in the *ND2* Subunit of Mitochondrial Complex I Are Sufficient to Confer Increased Tumorigenic and Metastatic Potential to Cancer Cells. Cancers (Basel). 211(7), 1027. Published 2019 Jul 21. doi:10.3390/cancers11071027.

Nakamura, T., Matsuoka, I., 1978. Calorimetric studies of heat of respiration of mitochondria. J. Biochem. 84 (1), 39–46. https://doi.org/10.1093/oxfordjournals.jbchem.a132117. PMID: 690103.

Nakano, M., Arai, Y., Kotera, I., Okabe, K., Kamei, Y., Nagai, T., 2017. Genetically encoded ratiometric fluorescent thermometer with wide range and rapid response. PLoS One 12 (2), e0172344.

Nath, S., 2016. The thermodynamic efficiency of ATP synthesis in oxidative phosphorylation. Biophys. Chem. 219, 69–74. https://doi.org/10.1016/j.bpc.2016.10.002.

Naučienė, Z., Zūkienė, R., Degutytė-Fomins, L., Mildažienė, V., 2012. Mitochondrial membrane barrier function as a target of hyperthermia. Medicina (Kaunas) 48 (5), 249–255. PMID: 22864272.

Nicholls, D.G., Ferguson, S.J., 2013. Quantitative Bioenergetics: The Measurement of Driving Forces. In: Nicholls, D.G., Ferguson, S.J. (Eds.), Bioenergetics 4, Academic Press, pp. 27–51.

Okabe, K., Sakaguchi, R., Shi, B., Kiyonaka, S., 2018. Intracellular thermometry with fluorescent sensors for thermal biology. Pflügers Archiv - *European Journal of Physiology* 470, 717–731. https://doi.org/10.1007/s00424-018-2113-4.

Patron, M., Tarasenko, D., Nolte, H., et al., 2022. Regulation of mitochondrial proteostasis by the proton gradient. EMBO J 41 (16), e110476. https://doi.org/10.15252/embj.2021110476.

Pryde, K.R., Taanman, J.W., Schapira, A.H., 2016. A LON-ClpP Proteolytic Axis Degrades Complex I to Extinguish ROS Production in Depolarized Mitochondria. Cell Rep. 17 (10), 2522–2531. https://doi.org/10.1016/j.celrep.2016.11.027. PMID: 27926857; PMCID: PMC5177631.

Qian, L., Song, X., Ren, H., Gong, J., Cheng, S., 2004. Mitochondrial mechanism of heat stress-induced injury in rat cardiomyocyte. Cell Stress Chaperones 9 (3), 281–293. https://doi.org/10.1379/csc-20r.1. PMID: 15544166; PMCID: PMC1065287.

Qiao, J., Chen, C., Shangguan, D., Mu, X., Wang, S., Jiang, L., Qi, L., 2018. Simultaneous Monitoring of Mitochondrial Temperature and ATP Fluctuation Using Fluorescent Probes in Living Cells. Anal. Chem. 90 (21), 12553–12558. https://doi.org/10.1021/acs.analchem.8b02496.

Rolfe, D.F.S., Brown, G.C., 1997. Cellular energy utilization and molecular origin of standard metabolic rate in mammals. Physiol. Rev. 77, 731–758. https://doi.org/10.1152/physrev.1997.77.3.731.

Roti Roti, J.L., 2008. Cellular responses to hyperthermia (40–46 degrees C): cell killing and molecular events. Int. J. Hyperth. 24 (1), 3–15. https://doi.org/10.1080/02656730701769841. PMID: 18214765.

Rugolo, M., Zanna, C., Ghelli, A.M., 2021. Organization of the Respiratory Supercomplexes in Cells with Defective Complex III: Structural Features and Metabolic Consequences Published 2021 Apr 17 Life (Basel) 11 (4), 351. doi: 10.3390/life11040351.

Sakaguchi, R., Kiyonaka, S., Mori, Y., 2015. Fluorescent sensors reveal subcellular thermal changes. Curr. Opin. Biotechnol. 31, 57–64. https://doi.org/10.1016/j.copbio.2014.07.013.

Savchuk, O.A., Silvestre, O.F., Adão, R.M.R., Nieder, J.B., 2019. GFP fluorescence peak fraction analysis based nanothermometer for the assessment of exothermal mitochondria activity in live cells. Sci. Rep. 9, 1–11. https://doi.org/10.1038/s41598-019-44023-7.

Šilkūnienė, G., Žūkienė, R., Naučienė, Z., Degutytė-Fomins, L., Mildažienė, V., 2018. Impact of Gender and Age on Hyperthermia-Induced Changes in Respiration of Liver Mitochondria. Medicina (Kaunas) 54 (4), 62. https://doi.org/10.3390/medicina54040062. PMID: 30344293; PMCID: PMC6174333.

Slimen, I.B., Najar, T., Ghram, A., Dabbebi, H., Ben Mrad, M., Abdrabbah, M., 2014. Reactive oxygen species, heat stress and oxidative-induced mitochondrial damage. A review, *International Journal of Hyperthermia* 30 (7), 513–523. https://doi.org/10.3109/02656736.2014.971446.

Strober, W., 2001. Trypan Blue Exclusion Test of Cell Viability. Curr. Protoc. Immunol. 21 https://doi.org/10.1002/0471142735.ima03bs21.

Wilkening, A., Rüb, C., Sylvester, M., Voos, W., 2018. Analysis of heat-induced protein aggregation in human mitochondria. J. Biol. Chem. 293(29), 11537-11552. doi: 10.1074/jbc.RA118.002122. Epub 2018 Jun 12. PMID: 29895621; PMCID: PMC6065183.

Willis, W.T., Jackman, M.R., Bizeau, M.E., Pagliassotti, M.J., Hazel, J.R., 2000. Hyperthermia impairs liver mitochondrial function in vitro. Am. J. Physiol. Regul. Integr. Comp. Physiol. 278 (5), R1240–R1246. https://doi.org/10.1152/ajpregu.2000.278.5.R1240. PMID: 10801293.

Wittig, I., Schägger, H., 2008. Features and applications of blue-native and clear-native electrophoresis. Proteomics 8 (19), 3974–3990. https://doi.org/10.1002/pmic.200800017.

Wust, P., Hildebrandt, B., Sreenivasa, G., Rau, B., Gellermann, J., Riess, H., et al., 2002. Hyperthermia in combined treatment of cancer. Lancet Oncol 3 (8), 487–497. https://doi.org/10.1016/s1470-2045(02)00818-5.

Yu, T., Ferdjallah, I., Elenberg, F., Chen, S.K., Deuster, P., Chen, Y., 2018. Mitochondrial fission contributes to heat-induced oxidative stress in skeletal muscle but not hyperthermia in mice. Life Sci. 1 (200), 6–14. https://doi.org/10.1016/j.lfs.2018.02.031. Epub 2018 Feb 27 PMID: 29499282.

Zhao, Q.L., Fujiwara, Y., Kondo, T., 2006. Mechanism of cell death induction by nitroxide and hyperthermia. Free Radic. Biol. Med. 40 (7), 1131–1143. https://doi.org/10.1016/j.freeradbiomed.2005.10.064. Epub 2005 Nov 22 PMID: 16545680.

Zukiene, R., Nauciene, Z., Ciapaite, J., Mildaziene, V., 2010. Acute temperature resistance threshold in heart mitochondria: Febrile temperature activates function but exceeding it collapses the membrane barrier. Int. J. Hyperth. 26 (1), 56–66. https://doi.org/10.3109/02656730903262140. PMID: 20100053.

Žūkienė, R., Naučienė, Z., Šilkūnienė, G., Vanagas, T., Gulbinas, A., Zimkus, A., Mildažienė, V., 2017. Contribution of mitochondria to injury of hepatocytes and liver tissue by hyperthermia. Medi*cina (Kaunas)*. 53 (1), 40–49. https://doi.org/10.1016/j.medici.2017.01.001. Epub 2017 Jan 9 PMID: 28256298.

Zurawa-Janicka, D., Jarzab, M., Polit, A., Skorko-Glonek, J., Lesner, A., Gitlin, A., et al., 2013. Temperature-induced changes of HtrA2(Omi) protease activity and structure. Cell Stress Chaperones. 18(1), 35-51. doi: 10.1007/s12192-012-0355-1. Epub 2012 Aug 1. PMID: 22851136; PMCID: PMC3508124.